

Evolution of Complex Phases in Al-Fe-Si Systems

Juraj Zigo^{a*}, Peter Svec^a, Dusan Janickovic^a, Irena Janotova^a,

Igor Matko^a, Marek Mihalkovic^a, Peter Svec Sr^a

^aInstitute of Physics, Slovak Academy of Sciences – SAV, Dubravská cesta 9, 845 11 Bratislava, Slovakia

Received: October 27, 2014; Revised: July 9, 2015

Phase transformations and composition of Al-Fe-Si, Al-Co-Si and Al-Ni-Si based rapidly quenched ribbons have been investigated. Different Al-Si based alloys with varying Si content and additions of third metallic element, namely $\text{Al}_{80}\text{Si}_{20}$, $\text{Al}_{60}\text{Si}_{40}$, $\text{Al}_{75}\text{Fe}_5\text{Si}_{20}$, $\text{Al}_{70}\text{Fe}_{10}\text{Si}_{20}$, $\text{Al}_{75}\text{Co}_5\text{Si}_{20}$, $\text{Al}_{70}\text{Co}_{10}\text{Si}_{20}$, $\text{Al}_{75}\text{Ni}_5\text{Si}_{20}$, $\text{Al}_{70}\text{Ni}_{10}\text{Si}_{20}$ were analyzed. Variation of phase composition with elemental composition was observed. Evolution of phases was determined by resistometry, differential scanning calorimetry (DSC). In situ X-ray diffraction (XRD) and transmission electron microscope (TEM) records were observed during isothermal and isochronal annealing.

Keywords: metallic glasses, planar flow casting, amorphous materials, aluminum-silicon alloys, nanocrystalline structure

1. Introduction

Conventional aluminum alloys are widely used for good mechanical properties and relatively light weight. Enhancing these properties could be made by alloying aluminum with various elements such as silicon, which is reasonable choice in terms of sustaining light weight properties. Producing Al-Si alloy with higher silicon content cannot be achieved by conventional metallurgy. Even by rapid quenching, only up to few weight percent of Si content has been attained in binary Al-Si alloys. It was found that increasing content of dissolved silicon is possible by adding other alloying components. Candidates with respect to low specific mass are transition elements of 4th period (from scandium to zinc).

We have chosen to investigate rapidly quenched alloys of Al-Si with transition elements (T) iron, cobalt and nickel. Composition of the investigated systems was $\text{Al}_{80-x}\text{T}_x\text{Si}_{20}$ where T = Fe, Co, Ni and x = 0, 5 and 10.

2. Experimental Details

Rapidly quenched ribbons consisting of Al-Si, Al-Fe-Si, Al-Co-Si and Al-Ni-Si (namely $\text{Al}_{80}\text{Si}_{20}$, $\text{Al}_{60}\text{Si}_{40}$, $\text{Al}_{75}\text{Fe}_5\text{Si}_{20}$, $\text{Al}_{70}\text{Fe}_{10}\text{Si}_{20}$, $\text{Al}_{75}\text{Co}_5\text{Si}_{20}$, $\text{Al}_{70}\text{Co}_{10}\text{Si}_{20}$, $\text{Al}_{75}\text{Ni}_5\text{Si}_{20}$, $\text{Al}_{70}\text{Ni}_{10}\text{Si}_{20}$) have been prepared by the planar flow casting (PFC) technique. During PFC, the melt is pressed by gas pressure through a nozzle on a surface of a fast rotating copper wheel. This allows the melt to solidify in a very short time of few μs . Final product obtained this way is a 20-40 μm thick amorphous, or in some cases nanocrystalline or polycrystalline ribbon with widths ranging from few mm to tens of mm. This structure can be further heat treated, while observing its physical properties. Changes in physical properties such as relative electrical resistivity and heat evolution are indicators of ongoing phase transformations. Structural properties before, during and after heat treatment can be for example observed by

X-ray diffraction, transmission electron microscopy (TEM) or electrical resistivity measurements.

Change of resistivity of the ribbons was measured during linear heating. Relative resistivity was acquired using resistivity bridge (Linear Research LR-100). Samples were heat treated in planar furnace with high spatial uniformity of temperature in argon atmosphere.

Differential scanning calorimetry was used to determine heat flow during linear heating of samples using DSC Perkin-Elmer 8500.

Eventual variation of magnetic properties with heating was examined by thermogravimetric analysis using Perkin-Elmer TGA 7 with a small magnet (~20 mT).

Content of various phases in samples was examined using X-ray diffraction or in-situ X-ray diffraction. Samples have been examined in as-cast state, after heat treatment or during linear heating using Bruker D8 Advance powder diffractometer with Cr K-alpha radiation. In-situ XRD patterns were obtained sequentially during linear heating.

Microstructure of samples was investigated using in-situ transmission electron microscopy (JEOL 2000FX at 200 kV). Micrographs were obtained during linear heating of sample in hot stage. Electron diffraction was used to determine phases present in the as-quenched state or during heat treatment.

3. Results

Samples in as-quenched state were analyzed by XRD to determine their state and phase composition.

Figure 1 shows diffraction patterns of Al-Fe-Si, Al-Co-Si, Al-Ni-Si and Al-Si alloys. Reference alloy $\text{Al}_{60}\text{Si}_{40}$ shows mainly content of fcc-Al and Si.

The content of Si phase significantly decreases already with addition of 5 at. % of transition element, as is clearly visible by the decreases of the intensity of Si diffraction

*e-mail: juraj.zigo@savba.sk

maxima. Specifically, $Al_{75}Co_5Si_{20}$ still shows content of mainly fcc-Al and Si phases, but the content of Si phase is decreased. We also detected content of various Al-Co and Al-Si phases, such as $Al_{0.52}Co_{0.48}$, $Al_{0.96}Co_{1.04}$ and $Al_{3.21}Si_{0.47}$. For $Al_{75}Fe_5Si_{20}$, we also detected fcc-Al phase, Si phase as well as a rather interesting $Al_{3.21}Si_{0.47}$ complex Al-based phase¹. Similar results were obtained for $Al_{75}Ni_5Si_{20}$, together with

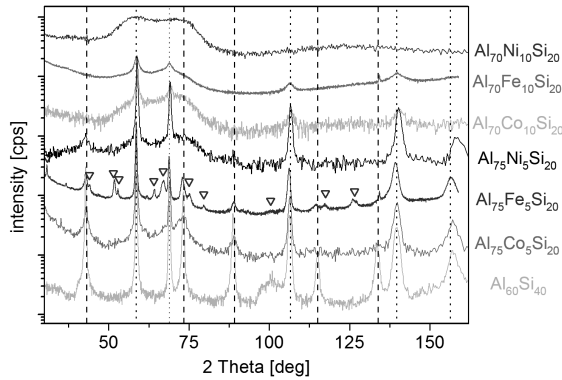


Figure 1. X-ray diffraction patterns of as-quenched alloys. Dotted lines mark fcc-Al phase peaks, dashed lines mark Si phase peaks. Upside-down triangles mark peaks of complex Al-based phases.

broader diffraction maxima, which suggest certain amount of amorphous or disordered phase.

Content of Si as a phase is decreased even more by adding 10 at.% of transition element. Phase composition becomes more simple and the content of amorphous phase is increased as demonstrated in Figure 1. Analysis of $Al_{70}Co_{10}Si_{20}$ and $Al_{70}Fe_{10}Si_{20}$ shows comparable results - amorphous plateau around 2θ angles $50-90^\circ$ and minor maxima assigned to crystalline fcc-Al. For $Al_{75}Ni_5Si_{20}$, bimodal broad plateau is present, which can be a signature of either ultrafine nanocrystalline grains of Al or of phase separation in amorphous state similar to that observed in bulk metallic glasses².

To examine alloy thermodynamic and reaction kinetic properties, relative electrical resistivity (Figure 2) and DSC measurements (Figure 3) during heating were performed. Alloys of $Al_{80}Si_{20}$ and $Al_{75}Co_5Si_{20}$ showed steep slope of $R(T)/R(300K)$ (high temperature coefficient of resistivity), which is evidence of polycrystalline structure.

Compared to that, alloys with composition of $Al_{75}Ni_5Si_{20}$, $Al_{70}Ni_{10}Si_{20}$ and $Al_{70}Co_{10}Si_{20}$ have much lower temperature coefficient of resistivity, for $Al_{70}Ni_{10}Si_{20}$ and $Al_{70}Co_{10}Si_{20}$ even with negative value. Complicated evolution of resistivity of $Al_{75}Ni_5Si_{20}$, $Al_{70}Ni_{10}Si_{20}$, and $Al_{70}Co_{10}Si_{20}$, is evidence of ongoing phase transformations from metastable state during

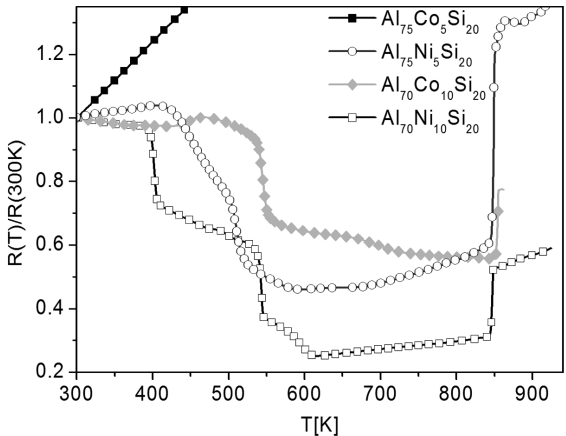
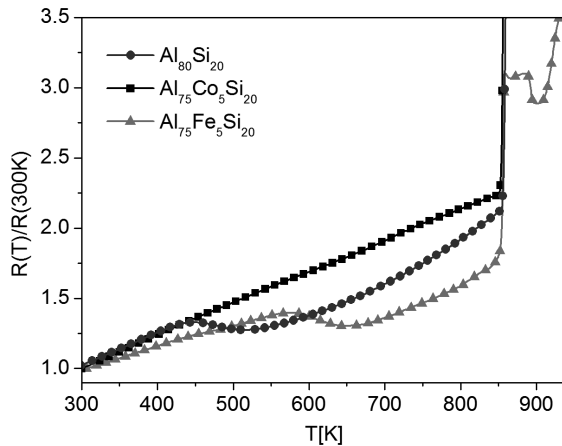


Figure 2. Temperature dependence of relative electrical resistivity (linear heating 10K/min).

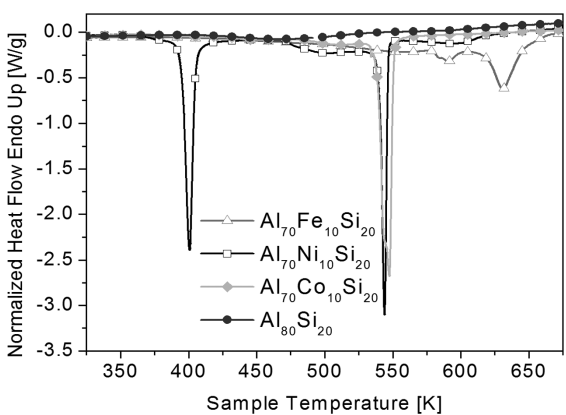
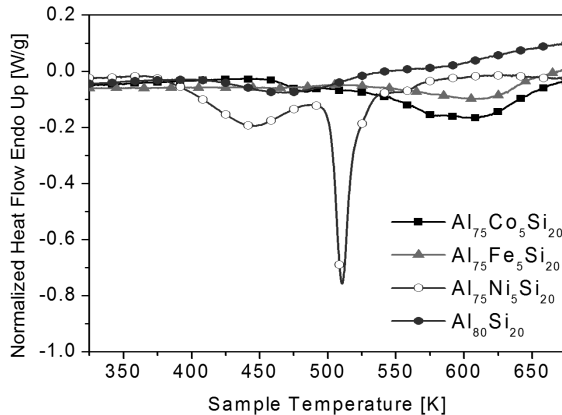


Figure 3. DSC measurement (linear heating 10K/min).

heating. Nearly vertical step present in all curves at high temperatures corresponds to melting of Al phase.

Subsequently to these measurements, we were interested in evolution of phases which might occur during phase transformations. In-situ XRD and TEM was used in this manner in order to map and image phase composition changes during heating.

In-situ TEM analysis was used for $\text{Al}_{75}\text{Ni}_5\text{Si}_{20}$ and $\text{Al}_{70}\text{Ni}_{10}\text{Si}_{20}$ alloys. These are the most interesting systems from the viewpoint of phase transformations and as-cast state. Phase composition changes during heat treatment occurred in both cases at temperatures expected from resistivity and DSC measurements (Figures 2 and 3). Micrographs of as-cast $\text{Al}_{75}\text{Ni}_5\text{Si}_{20}$ (Figure 4) shows mixed amorphous and crystalline phases, as was expected from the slope of resistivity curve. In as-cast state, amorphous-like regions surrounded by mixed amorphous and crystalline regions were observed.

These seem to be morphologically similar to structures referred to as q-glass, which were observed in rapidly quenched alloys of Al-Fe-Si. Q-glass is presumed to grow like a crystal, while being isotropic³. During heating to 500K (Figure 4b), growth of fcc-Al(Si,Ni) nanocrystals took place. With heating to 600K (Figure 4c) further growth of Al-grains and their coalescence took place. Continued heating between 600 and 800K (Figure 4d) lead to further coarsening of the fcc-Al phase and to formation of additional intermetallic phases.

In case of $\text{Al}_{70}\text{Ni}_{10}\text{Si}_{20}$, similar results were obtained. In as-cast state, two different types of morphology were observed. Figure 5a shows fine crystalline region without amorphous phase (consisting mainly of fcc-Al, Al_3Ni , NiSi_2

and Al_5Si), while Figure 5b shows amorphous region similar to that observed in $\text{Al}_{75}\text{Ni}_5\text{Si}_{20}$. During heating to 610K, phase transformations and growth of grains took place. With further heating to 800K, further coarsening of fcc-Al phases was observed with resulting Al_3Ni , Si and fcc-Al composition.

Evolution of phase composition of $\text{Al}_{70}\text{Fe}_{10}\text{Si}_{20}$, $\text{Al}_{70}\text{Ni}_{10}\text{Si}_{20}$ and $\text{Al}_{75}\text{Ni}_5\text{Si}_{20}$ was observed by in-situ XRD. XRD was cyclically measured in range of 2θ angles from 50° to 80° at temperatures from 320K to 850K. These measurements, displayed in Figure 6, clearly show transformations of XRD patterns at temperatures corresponding to transformation temperatures measured by DSC or relative resistivity measurement. $\text{Al}_{70}\text{Fe}_{10}\text{Si}_{20}$ (Figure 6a) in as-cast state shows partly amorphous structure mixed with fcc-Al phase (fcc-Al peaks are marked by black dotted lines). During heating, it transforms to form polycrystalline pattern with fcc-Al and Si peaks. $\text{Al}_{70}\text{Ni}_{10}\text{Si}_{20}$ (Figure 6b) is amorphous in as-cast state. During heating, it transforms in several stages to form fcc-Al and Al_3Ni phases⁴. $\text{Al}_{75}\text{Ni}_5\text{Si}_{20}$ (Figure 6c) transforms from mixed amorphous and crystalline (consisting mainly fcc-Al) state to form fcc-Al, Al_3Ni and Si phases.

More detailed view on how $\text{Al}_{70}\text{Ni}_{10}\text{Si}_{20}$ XRD pattern is changing with temperature is presented on Figure 7, which displays XRD patterns in as-cast state and annealed to selected temperatures from 448K to 763K.

To review potential (ferro)magnetic properties of alloys, M-TGA measurement have been made. Data acquired by this technique are displayed on Figure 8, which show nearly no variation of magnetic properties with temperature comparable to instrument baseline.

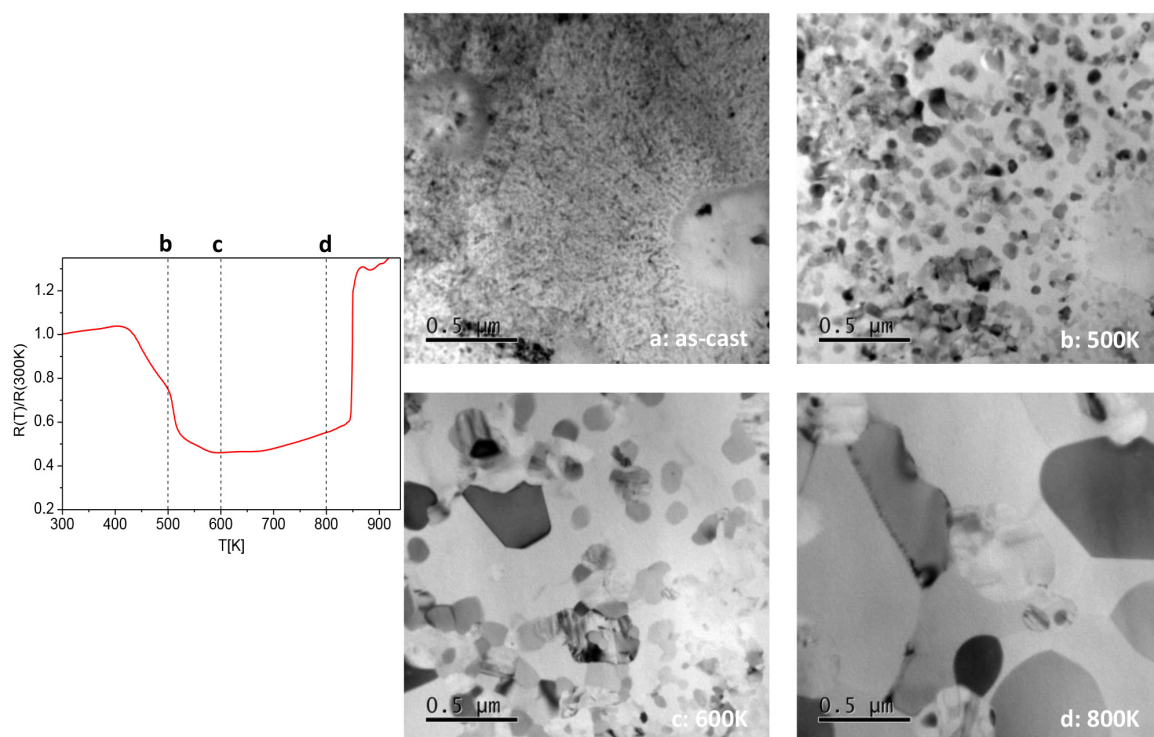


Figure 4. TEM micrographs of $\text{Al}_{75}\text{Ni}_5\text{Si}_{20}$ alloy in as-cast state (a), and during in-situ heat treatment at 500K (b), 600K (c) and 800K (d).

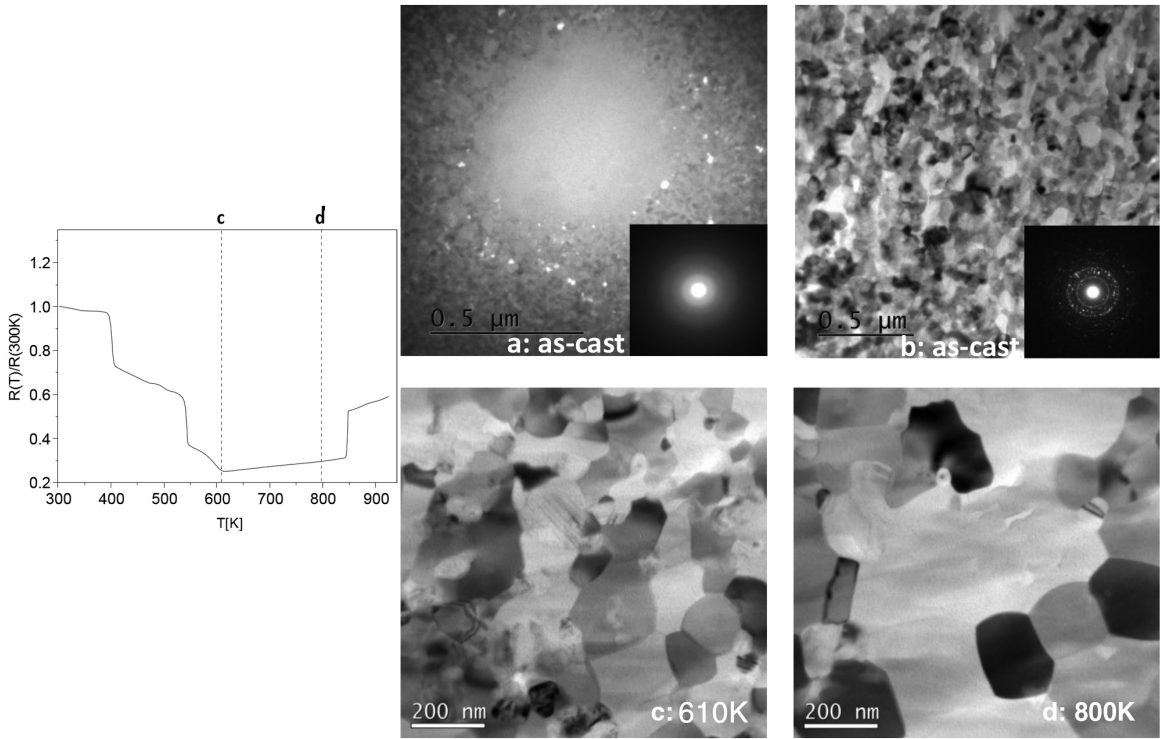


Figure 5. TEM micrographs of $Al_{75}Ni_{10}Si_{20}$ alloy in as-cast state (a), and during in-situ heat treatment at 500K (b), 600K (c) and 800K (d).

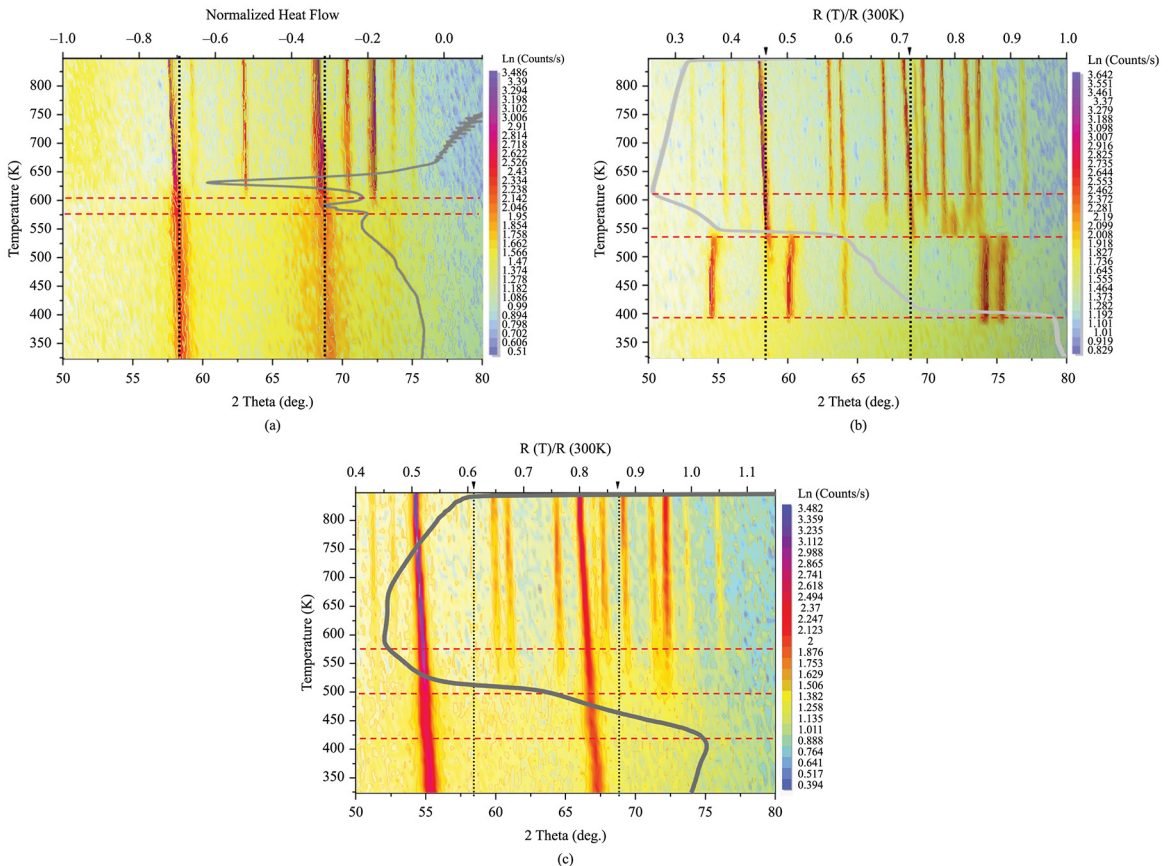


Figure 6. Overview of XRD patterns of $Al_{70}Fe_{10}Si_{20}$ (a), $Al_{70}Ni_{10}Si_{20}$ (b) and $Al_{75}Ni_{10}Si_{20}$ (c) alloys during heat treatment from as-cast state to 853K. Inset shows DSC curve (a) and resistivity curve (b and c). Dotted lines mark fcc-Al phase peaks.

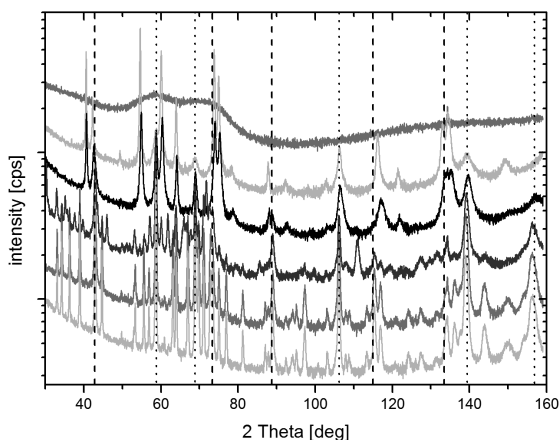


Figure 7. XRD patterns of $\text{Al}_{75}\text{Ni}_{10}\text{Si}_{20}$ alloy in as-cast state, and during heat treatment at temperatures from 448K to 763K. Dotted lines mark fcc-Al phase peaks, dashed lines mark Si phase peaks.

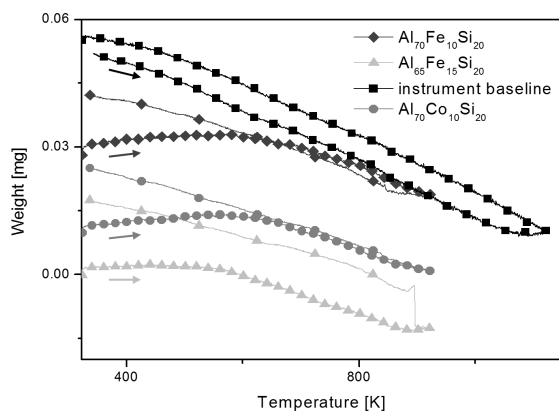


Figure 8. M-TGA measurement of alloys (linear heating 10K/min). Arrows mark heating parts of curves, cooling curves are without arrows.

References

1. Long GG, Chapman KW, Chupas PJ, Bendersky LA, Levine LE, Momprou F, et al. Highly ordered noncrystalline metallic phase. *Physical Review Letters*. 2013; 111(1):015502. <http://dx.doi.org/10.1103/PhysRevLett.111.015502>. PMID:23863012.
2. Park ES and Kim DH. Phase separation and enhancement of plasticity in Cu–Zr–Al–Y bulk metallic glasses. *Acta*

4. Conclusions

Rapidly quenched systems of Al-Si with addition of Fe, Ni or Co have been examined. Evolution of relative resistivity with temperature and DSC measurements were obtained to map phase transformations. To qualify phase composition before and after these transformations, phase composition in as-cast state and evolution of phase composition with temperature was observed by in-situ XRD and TEM.

Alloys with 5 at.% of transition element in as-cast state were composed mostly by fine crystalline fcc-Al and Si phases embedded in amorphous matrix. Interesting amorphous-like areas surrounded by crystalline phase were observed by TEM in initially metastable $\text{Al}_{75}\text{Ni}_{10}\text{Si}_{20}$, which disintegrated during heating. By increasing content of transition element to 10 at.%, mainly amorphous metastable phases were observed in as-cast state. In-situ XRD analysis of $\text{Al}_{70}\text{Fe}_{10}\text{Si}_{20}$ demonstrated high temperature stability of the initial phase up to approximately 575K. $\text{Al}_{70}\text{Ni}_{10}\text{Si}_{20}$ transforms at lower temperatures several times to form fcc-Al and Al_3Ni phases. Structure morphology and electron diffraction patterns of this sample were observed by in-situ TEM.

Incorporation of Si into other phases was achieved by rapid quenching of $\text{Al}_{80-x}\text{T}_x\text{Si}_{20}$ alloys (T = Fe, Ni, Co) with content of transition element (x) between 5 and 10 at.%. This can help to eliminate Si dendrites in Al-Si based alloys and potentially enhance mechanical properties.

Acknowledgements

This work was supported by the Slovak Scientific Grant Agency (VEGA 2/0189/14), Slovak Research and Development Agency (APVV-0492-11, APVV-0647-10, APVV-0076-11) and by the Center of Excellence for Functional Materials.

Materialia. 2006; 54(10):2597-2604. <http://dx.doi.org/10.1016/j.actamat.2005.12.020>.

3. Chapman KW, Chupas PJ, Long GG, Bendersky LA, Levine LE, Momprou F, et al. An ordered metallic glass solid solution phase that grows from the melt like a crystal. *Acta Materialia*. 2014; 62:58-68. <http://dx.doi.org/10.1016/j.actamat.2013.08.063>.
4. Yamamoto A and Tsubakino H. Al_9Ni_2 precipitates formed in an Al-Ni dilute alloy. *Scripta Materialia*. 1997; 37(11):1721-1725. [http://dx.doi.org/10.1016/S1359-6462\(97\)00329-1](http://dx.doi.org/10.1016/S1359-6462(97)00329-1).